JPMTR 069 | 1504
DOI 10.14622/JPMTR-1504
UDC 53.07 : 535.3 | 667.6

Original scientific paper
Received: 2015-08-10
Accepted: 2015-11-04

Modelling reflectance factor for special effect pigment coatings

Nina Rogelj[1] and Marta Klanjšek Gunde[2]

[1] University of Eastern Finland, Institute of Photonics, Joensuu, P.O.Box 111, Finland
E-mail: nina.rogelj@uef.fi

[2] National Institute of Chemistry, Ljubljana, Hajdrihova 19, Slovenia
E-mail: marta.k.gunde@ki.si

Abstract

A numerical model to calculate goniometric reflectance factor for effect coatings with interference flakes was developed and analysed here. The model incorporates three parts of the light scattering events; from the front surface of the coating, from pigments inside the coating, and from the coating substrate. In order to validate the model, reflectance spectra were measured at an incident angle of 45º and at reflected angles of −60º, −30º, −20º, 0º, 30º and 65º using a commercial multi-angle spectrometer. Metal lustre coating was used for testing the model. It contains Iriodin 4504 pigment, an interference mica-based pigment coated with iron (III) oxide from Merck. This coating includes all spectral characteristics involved in the model. The thickness of the interference layer on the pigments was adjusted to obtain good matches of interference features between modelled and measured reflectance factor. The influence of surface coverage by pigments and of the pigment orientation distribution on the resulting spectra was analysed. The first parameter represents the fraction of surface area covered with pigments and the second how well the pigments inside the coatings are oriented.

Keywords: appearance, scattering, spectrum, multi-angle reflectance, effect coating

1. Introduction and background

Surfaces that change their appearance significantly with illumination and viewing directions are becoming increasingly important in several applications, ranging from the purely decorative up to providing various functional purposes. The unique optical impressions of such surfaces give eye-catching effects, angle-dependent interference colours, pearl lustre, or multiple reflection, which characterize the appearance of the so-called gonioapparent effect. A large variety of samples falls into this class, giving angle-dependent effects due to (a) topography of the micro- and macro textures of surfaces, such as leather, textile and other microtextured surfaces, and (b) optical effects coming from metallic, interference and surface-structured flaky pigments applied in coatings, plastics and printing inks, which are mostly used in automotive, decorative and security coatings. The optical properties of such samples spread well beyond solid colour and cannot be described by any straightforward colorimetric measurement. Advanced applications demand production of surfaces with repeatable appearance, which requires controllable production process and possibility to predict the appearance. Several conditions have to be fulfilled for these requirements, such as the possibility to measure the appearance of such products, to identify the causes for differences among them, and to document these details in a convenient way. We have shown already that gonioospectrophotometric space curves, a special representation of the corresponding bidirectional reflectance distribution function (BRDF), could serve as an appearance fingerprint of several types of gonioapparent samples (Klanjšek Gunde and Rogelj, 2013). However, theoretical consideration of this methodology was made originally only on diffraction gratings (Rogelj, Poberaj and Klanjšek Gunde, 2013). For this purpose, the diffraction theory was applied to calculate the BRDF of diffraction gratings. This research is continued herein to analyse the numerical model that will enable reliable prediction of the BRDF of effect coatings, especially of paints or inks containing interference flakes.

BRDF contains spectral radiance coefficients for all possible illumination and viewing directions which could be measured by gonioreflectometry. Most research made so far has been done for metal-effect coatings, interference coatings, and more complex effect coatings. Three different geometries (i.e. combinations of illumination and viewing directions) are good enough for metallic coating (ASTM, 2001), whereas at least five or six geometries are required for coatings adopting the interference effect (Takagi, Watanabe and Baba, 2005). Most complex effect coatings require 1 485 geometries (Takagi,

Sato and Baba, 2007). The goniospectrophotometers currently available on the market have 6 (BYK-mac i, BYK Gardner), 19 (MA98, X-Rite) and 98 geometries (GK311/M, Zeiss) (Kirchner and Cramer, 2012).

Effect pigments can be classified into two groups, class (i) pigments that consist of only one optically homogeneous material (substrate-free pigments, e.g. metallic and pearlescent flakes) and class (ii) pigments that have a layered structure and consist of at least two optically different layered material (pigments with layer-substrate structure or multilayered pigments with or without a substrate, e.g. interference flakes). The class (i) pigments give rise to reflection and/or partial refraction from flakes, which in the corresponding coating make metallic or pearlescent effects, respectively. Interference flakes from class (ii) add the effect of interference in thin film layers, which contributes strong angle-dependent colour, which is added to the lustre and brilliance (Pfaff and Reynders, 1999; Maile, Pfaff and Reynders, 2005).

The objective set for this research is to make a good calculation model for BRDF of effect coatings with interference flakes, and to verify it by comparison with goniospectrometric measurements. Most attention was devoted to build the theoretical model that could enable one to vary the optical constituents of effect coatings – i.e. the type of flakes (in terms of refractive index and absorption coefficient), their pigment-volume concentration, size, average inclination angle inside the coating and the corresponding variance. The optical properties of the substrate were also allowed to vary. Some steps in solving this optical problem were already presented (Germer and Nadal, 2001). They were included here and developed further for the purpose of the application in hand. The first successful and promising results of the research are shown here together with the plans for the future. First, building of the numerical model is explained, and then its application is presented for a coating with layered interference flakes (class (ii)). For this purpose, a suitable sample was selected from a commercial set of samples; its reflectance was measured using handheld goniospectrometer and calculated by the built numerical model. Most parameters of the tested sample were provided by the producer. The most important exemption is orientation of flakes inside coating; it heavily influences the appearance and must be included in the numerical model. However, it is well known that measurement of flake orientation in coatings is far from straightforward (Kirchner an Houweling, 2009; Maile, Pfaff and Reynders, 2005; Pfaff and Reynders, 1999). Contrary, the influence of flake's inclination angle and variance to this angle on the goniometric reflectance is easily analysed by variation of the corresponding parameters in the numerical model. This is one among many advantages of the model.

2. Materials and methods

2.1 Samples

The Merck Effect Pigments colour card (Merck-Gruppe, Darmstadt, Germany) was taken here as a source of effect coating with different pigments. A representative from the coatings with metal lustre pigments was selected. It contains Iriodin 4504 pigments (MERCK, 2012), which are interference pigments, consisting of mica-based flakes with thin layer of iron (III) oxide (Fe_2O_3). The coating is applied on a white subsurface; its appearance at measurement conditions is shown in Figure 1.

2.2 Measurements

The MA98 multiangle spectrometer (X-Rite, Inc.) was applied for measurements. The device is intended for analyses of most optically complex coatings, also on curved surfaces. It enables reflectance factor measurements within 19 geometries; two illumination directions, 45° and 15°, combined with 10 and 9 viewing directions, respectively. Four directions at each illumination are out of the plane of incidence, therefore there are 8 off-plane and 11 in-plane geometries. Angular accuracy of the equipment is ±1.15°, its reproducibility on average is 0.18 ΔE^*_{ab} on reference Series II BCRA tile set, and its repeatability, using 20 measurements at 5 seconds intervals, is maximum 0.03 ΔE^*_{ab} on white cal plaque (X-Rite, 2010). Measurements are taken at different locations on the sample to achieve average of 2 measurement values. The spectra were measured in the 400–700 nm spectral region with 10 nm increment. Only the in-plane measurements at 45° incident angle were analysed here. This

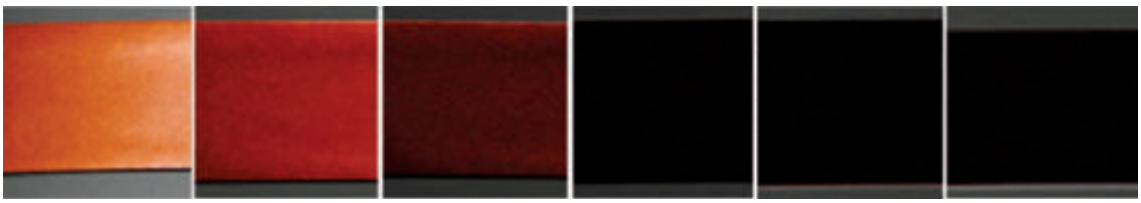

Figure 1: Photographs of the selected sample taken with 45° illumination angle in directions −60°, −30°, −20°, 0°, 30° and 65° (from left to right) in respect to surface normal; the in-plane geometry is used

gives 6 detection directions, −60°, −30°, −20°, 0°, 30° and 65°, as measured in respect to the surface normal. While the interference pigments in the selected sample are oriented uniformly and parallel to the substrate, the goniometric reflectance factor is distributed symmetrically around the in-plane direction, therefore, such a simplification is reasonable.

Reflection coefficients for paper substrates, which are used in the numerical model, were calculated from their reflectance factors. The latter were measured using a spectrophotometer Perkin Elmer λ 1050.

2.3 Calculations

The numerical model describes the scattering of light impinging onto a special effect pigment coating (Figure 2) at an incident angle θ_i from the surface normal. Reflection of scattered light is described using polar angle θ_r and azimuthal angle Φ_r relative to the normal to the flat surface of the coating. Pigments are assumed to be tilted at an angle θ_n'. Orientation distribution function describes how the tilt angle changes from flake to flake; it can be described by many functions. In this paper we use a logistic orientation distribution function P using θ_0' as a mean flake tilt angle and σ' as a standard deviation:

$$\mathrm{P}(\theta_\mathrm{n}', \theta_0', \sigma') = \frac{\exp\left(\frac{\theta_\mathrm{n}' - \theta_0'}{\sigma'}\right)}{\sigma'\left(1+\exp\left(\frac{\theta_\mathrm{n}' - \theta_0'}{\sigma'}\right)\right)^2}\mathrm{C} \qquad [1]$$

In Equation [1], C is the fraction of the surface area which is covered by pigments, going from 0 (no pigments) to 1 (pigments cover the whole sample area). Other angles in Equation [1] describe the applied geometry as shown in Figure 2.

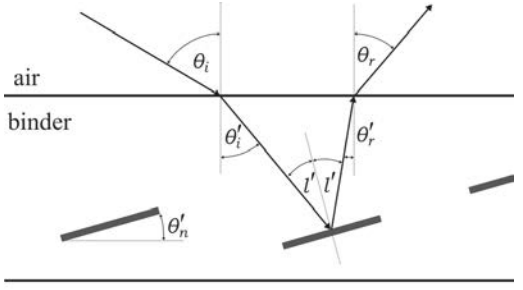

Figure 2: Simplified schematic of light scattering on special effect pigment coating

2.3.1 Numerical model

The numerical model presented in this paper incorporates three models, named here as facet model, flake model, and base model. Each of the models describes scattering from different level of the coating with special effect pigments:

- scattering from front surface of the coating – facet model
- scattering from special effect pigments inside the coating – flake model
- scattering from substrate of the coating – base model

Scattering from the whole sample is then described using Stokes vector S:

$$S = (F^{facet}G + F^{flake}G + F^{base})S_0 \qquad [2]$$

where $F^{facet}/F^{flake}/F^{base}$ are the Mueller matrices BRDF for the facet/flake/base model respectively, S_0 is the Stokes vector of the incident light, and G is the geometrical attenuation factor, which accounts for masking and shadowing of the light at large reflection angles. Its definition and formulation can be found in Torrance and Sparrow (1967). The facet and flake models are treated in similar way and are described in detail in Germer and Nadal (2001), and in Germer, Zwinkels and Tsai (2014). They are used to calculate F^{facet} and F^{flake} by following the equation:

$$F = \frac{P}{4\cos\theta_i \cos\theta_r \cos\theta_n} M \qquad [3]$$

using different Mueller matrices, M^{facet} and M^{flake}, appropriate angles (θ_i, θ_r, θ_n or θ_i', θ_r', θ_n'), and orientation distribution function (P). The facet model treats the scattering from the front surface as a specular reflection from the aligned facets which have their slopes distributed according to the orientation distribution function. The flake model treats pigments as aligned facets and also takes into account the refraction into and out of the binder, surrounding the flakes. The facet and flake models are presented more in depth in Germer and Nadal (2001), and in Germer, Zwinkels and Tsai (2014), whereas the base model is described in the next subsection.

2.3.2 Base model

Scattering from the substrate is incorporated in the base model. According to this model, light can take four different paths on its way through the coating towards the substrate and back. The paths, along with the corresponding angle notations are schematically represented in Figure 3, and expressed as:

1. transmission through pigments, diffuse reflection from substrate, transmission returning through pigments,
2. transmission through pigments, diffuse reflection from substrate, transmission returning through binder (no crossing of pigments),

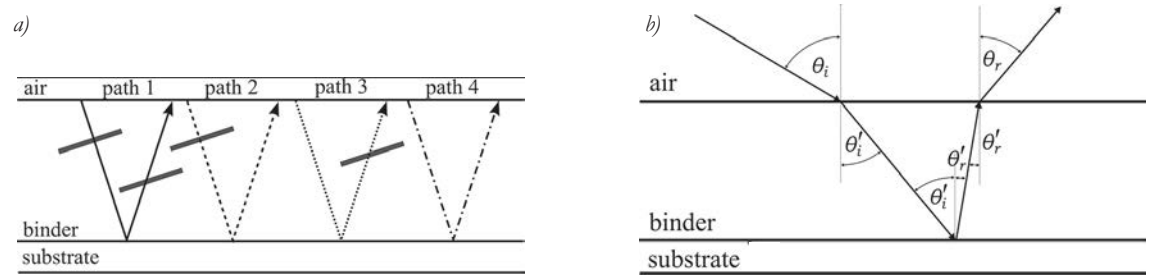

Figure 3: a) Schematic representation of the four different paths the light can follow when undergoing scattering from the substrate, where for simplicity only few pigment flakes are drawn, and b) schematic representation of angles used in the base model

3. transmission through binder (no crossing of pigments), diffuse reflection from substrate, transmission returning through pigments,
4. transmission through binder (no crossing of pigments), diffuse reflection from substrate, transmission returning through binder (no crossing of pigments).

In Figure 3b, only the path 4 is shown. For other three paths, the angles are the same; we only add pigment on the corresponding side(s).

The path 1 will always occur to some extent, being the only possible path in the case of complete coverage ($C=1$), whereas the other three can occur only if $C<1$. Mueller matrices BRDF for the four different paths are calculated as:

$$F^{path\,1} = \frac{P(\theta_n', \theta_0', \sigma')n^2{}_{binder}}{4\cos\theta_i \cos\theta_r \cos\theta_n'} M^{path1} \quad [4a]$$

$$F^{path\,2} = \frac{P(\theta_n', \theta_0', \sigma')n^2{}_{binder}}{4\cos\theta_i \cos\theta_r \cos\theta_n'} (1-C) M^{path\,2} \quad [4b]$$

$$F^{path\,3} = \frac{P(\theta_n', \theta_0', \sigma')n^2{}_{binder}}{4\cos\theta_i \cos\theta_r \cos\theta_n'} (1-C) M^{path\,3} \quad [4c]$$

$$F^{path\,4} = (1-C)^2 M^{path\,4} \quad [4d]$$

and Mueller matrices are transformed from Jones matrices, J^{path}, as (Goldstein, 2003):

$$M = UJ \otimes J^* / U \quad [5a]$$

$$U = \frac{1}{\sqrt{2}} \begin{bmatrix} 1 & 0 & 0 & 1 \\ 1 & 0 & 0 & -1 \\ 0 & 1 & 1 & 0 \\ 0 & i & -i & 0 \end{bmatrix} \quad [5b]$$

Jones matrices for the four different paths are calculated as:

$$J^{path\,1} = \begin{bmatrix} q_{11}^{flake} t_s'^2(l') & q_{12}^{flake} t_s'(l') t_p'(l') \\ q_{21}^{flake} t_s'(l') t_p'(l') & q_{22}^{flake} t_p'^2(l') \end{bmatrix} \quad [6a]$$

$$J^{path\,2} = \begin{bmatrix} q_{11}^{flake} t_s'(l') & q_{12}^{flake} t_p'(l') \\ q_{21}^{flake} t_s'(l') & q_{22}^{flake} t_p'(l') \end{bmatrix} \quad [6b]$$

$$J^{path\,3} = \begin{bmatrix} q_{11}^{flake} t_s'(l') & q_{12}^{flake} t_p'(l') \\ q_{21}^{flake} t_p'(l') & q_{22}^{flake} t_s'(l') \end{bmatrix} \quad [6c]$$

$$J^{path\,4} = \begin{bmatrix} t_s(\theta_i) t_s(\theta_r) r_s''(l') & 0 \\ 0 & t_p(\theta_i) t_p(\theta_r) r_p''(l') \end{bmatrix} \quad [6d]$$

where q_{ij}^{flake} are elements of Jones matrix for facet model, t_s' and t_p' are transmission and r_s'' and r_p'' reflection coefficients for substrate and pigments, respectively. Transmission coefficients for pigments are calculated using the thicknesses of the pigment's layers and their wavelength-dependent refractive indices. The equations are well known and can be found, for example, in Germer, Zwinkels and Tsai (2014).

4.1 Numerical modelling of the samples

The described numerical model was used to calculate the reflectance factor of the selected sample at the conditions used for measurements. This includes six in-plane reflectance directions with 45° illumination and aspecular angles −60°, −30°, −20°, 0°, 30°, 65° as specified for MA98 multiangle spectrometer. The sample was described with a coating containing flaky pigments in a resinous binder (Table 1). A white paper was used as a substrate. The mica-based flakes, having thin interference layer made of Fe_2O_3 on both sides (Iriodin 4504, Merck) were used. The flakes are described as layer-core-layer where the corresponding thicknesses were adjusted by the best fit to the measured reflectance. Because the flakes cover the entire surface, $C=1$ was used. Vast majority of flakes were oriented parallel to the substrate, therefore the flake's mean tilt angle was taken to be $\theta_0'=0°$. The refractive index of SiO_2 was used instead of mica ($KAl_2(Si_3Al)O_{10}(OH,F)_2$). The refractive indices

of SiO_2, Fe_2O_3 and acrylic pitch (binder) were obtained from the literature (Palik, 1997; Kasarova et al., 2007; Database of AIU Jena, 2015), while the thicknesses of the core material and of the interference layer of flakes were obtained by the best match between the calculated and measured spectra, based on CIE76 colour difference (Schanda, 2007). The Stokes vector of the incident light for all calculations was that of an unpolarized light.

Table 1: Specifications of the analysed effect coating: data for the binder, the substrate and the flakes, where C is the coverage of the substrate by flakes, θ_0' is the flake's mean tilt angle and σ' is the standard deviation for the orientation distribution of flakes, binder layer thickness was estimated from measurements with caliper and flake's thicknesses were adjusted by the best fit to the measured reflectance while the mean diameter was taken from the Merck Effect Pigments colour cart

Binder	Material	acrylic pitch
	Layer thickness	600 μm
Substrate	Material	white paper
Special effect pigments (flakes)	Materials	Fe_2O_3 + mica + Fe_2O_3
	Thicknesses	(0.074 + 0.121 + 0.074) μm
	Mean diameter	5–50 μm
	C	1
	θ_0	0°
	σ'	3°

5. Results and discussion

The suitability of the numerical model to describe the goniometric reflectance factor of an effect coating was analysed in four steps. First, the measured reflectance factor was compared to the calculated one for the entire set of illumination–viewing angles. The thickness of the pigment flakes, the mica core and interference layer applied over it, were varied for the best possible match of the reflectance spectra. Second, the influence of the fraction of the substrate surface covered by pigments (parameter C in the Equation [1]) on the calculated reflectance factor was analysed. Third, the consequences of the orientation distribution function of flakes within coating were analysed. And fourth, the effect of different coloured paper substrates was analysed.

5.1 Measured vs. modelled reflectance factor

The calculations were made for the 440–700 nm spectral region because the published values for refractive index and absorption coefficient are limited to this region, and no extrapolation was made. Figure 4 shows the measured and calculated reflectance spectra for all applied illumination-viewing combinations and the corresponding CIELAB a^* and b^* colour values (Schanda, 2007) determined from the measured reflectance factor. The parameters used in computations are those from Table 1. The CIELAB values a^* and b^* are the largest at 60° reflectance angle and almost linearly diminish when this angle changes towards smaller and then negative values, where the appearance of the sample is going towards black. This is in accordance with photographs shown in Figure 1.

The measured spectra have a slight increase in reflectance at 440 nm, a valley between 500 and 550 nm, a peak around 630 nm and a decrease at 700 nm. The reader should notice that the measurements, as well as the model, provide reflectance factor and not reflectance. By definition, the reflectance factor is the ratio of radiant flux reflected of a sample in a given direction to that reflected in the same direction by perfectly reflecting diffuser (PRD). This means that some samples can reflect more light in a certain direction than the PRD, resulting in reflectance factor values above 1. The position of peaks and valleys is greatly determined by the thickness of interference layer applied on the mica core of the pigment flakes. The thickness data are not available for the Iriodin 4504 pigment, however, the percentage of each material used in the pigment is specified by the producer. The interference layer thickness and the thickness of the mica core were adjusted, using the percentage information, in order to minimize the colour difference, ΔE^*_{ab}, between the measured and calculated reflectance factor. The CIE76 colour-difference formula was applied for this purpose. Table 2 shows the results obtained for the spectra shown in Figure 4. The spectra show an acceptable match, however, the individual colour differences are quite large. The possible reasons

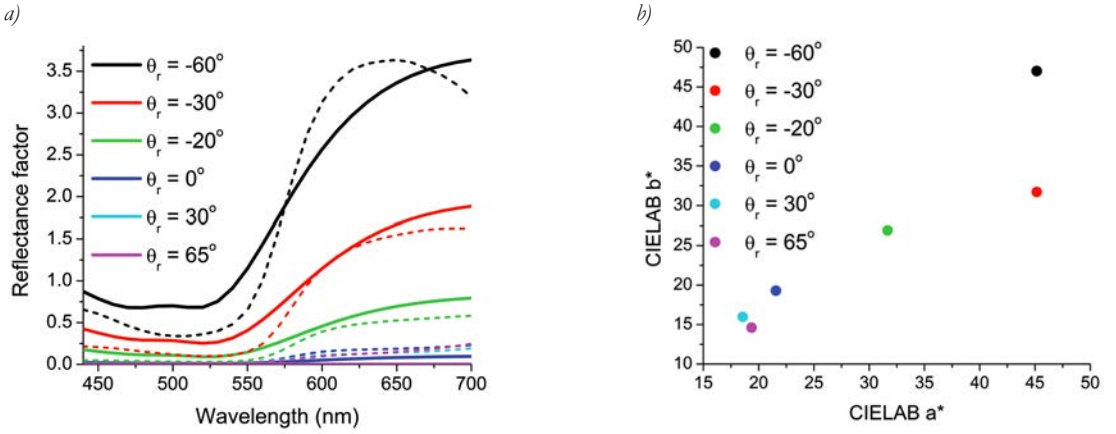

Figure 4: a) Measured (dashed line) and modelled (solid line) reflectance factor obtained for the selected coating sample with interference flakes and (b) CIELAB a and b* colour values calculated from the measured reflectance spectra (see also Figure 1 and Table 2); measurement directions are specified in the legend*

Table 2: CIE76 colour difference and RMSE between measured and modelled reflectance factor values

Aspecular angle	ΔE^*_{ab}	*RMSE*
−60°	20.58	0.3543
−30°	14.76	0.1702
−20°	12.32	0.1245
0°	17.64	0.0741
30°	26.29	0.0952
65°	26.27	0.1077

could be insufficient knowledge about the layers thicknesses, substituting optical constants of mica layer for optical constants of SiO_2, and insufficient modelling of the roughness of the mica flakes. Alongside the colour difference, Table 2 also shows the root mean square error (*RMSE*) between measured and calculated spectra. It was calculated as:

$$RMSE = \sqrt{\frac{\sum_{\lambda=440}^{700}(s_{\lambda,measured} - s_{\lambda,calculated})^2}{w}} \qquad [6]$$

where s represents reflectance spectra and w is the number of wavelengths.

5.2 Influence of surface coverage

Changing the volume concentration of pigments or their diameter, in general, changes the surface coverage, which is expressed by C in Equation [1]. Smaller surface coverage means that less of the area is covered with pigments and the substrate has a greater influence on the reflectance of such a sample. The influence of this effect on the reflectance factor spectra was analysed by calculating the reflectance factor spectra for all the applied illumination–viewing geometries using different values of the surface coverage, C. Figure 5 shows the results for C values of 0.1, 0.5 and 0.9. Smaller surface coverage results in bigger influence of the substrate, as expected. At wavelength below 530 nm, the reflectance factor in all viewing angles converges to a single value, but their relative separation stays the same as it is at longer wavelengths. The shape and the intensity of the reflectance factor changes with surface coverage. For smaller coverage, the reflectance factor becomes similar to that of the coating substrate alone (see also Figure 10). Therefore, the interference effect caused by the pigments is clearly seen at large enough coverage. This confirms the validity of the used computational model and enables to predict the concentration of flakes that should be used in coating if hiding of the substrate is desired.

The reader should pay special attention to the scale of the reflectance factor in Figure 5. When surface coverage is 1, the interference effect produces reflectance factor values higher than 1. With the smaller surface coverage, the interference effect diminishes and the reflectance factor values slowly became more similar to the reflectance factor of the substrate, meaning that the values go below 1.

5.3 Influence of orientation distribution function

The orientation distribution function of flakes is assumed to be a logistic distribution with its mean value, θ_0', and standard deviation, σ'. Since both parameters influence the results, we will analyse how each of them affects the reflectance spectra.

5.3.1 Influence of orientation distribution's standard deviation

Here, we assume that the mean tilt angle is 0°, meaning the flakes are parallel to the substrate, and we change

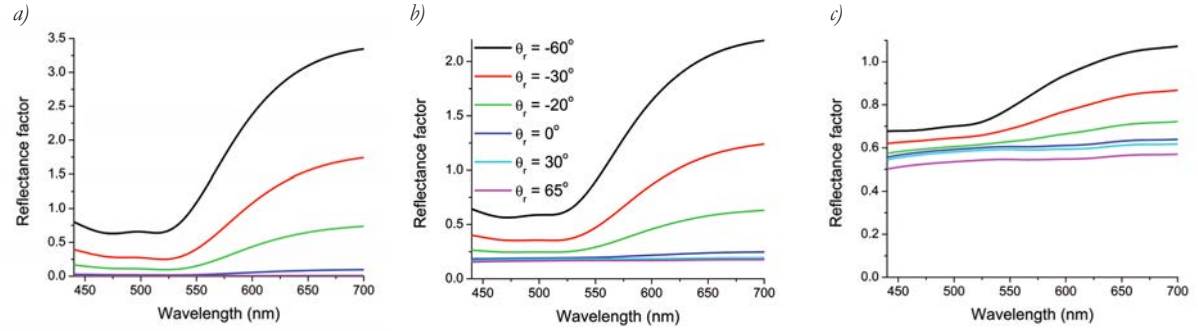

Figure 5: Reflectance factor spectra calculated for the applied illumination–viewing directions using surface coverage a) C = 0.9, b) C = 0.5, and c) C = 0.1; the legend in the middle graph is applicable to all three graphs

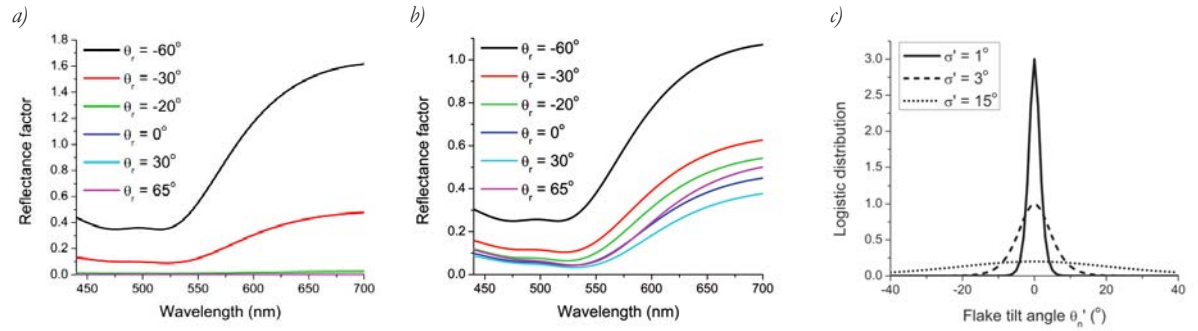

Figure 6: Reflectance factor spectra calculated for the applied illumination–viewing directions (see the legend) using surface coverage C = 1, the flake's mean tilt angle $\theta_0' = 0°$ and standard deviation of the orientation distribution function equal to a) σ' = 1° and b) σ' = 15°; the reader should pay attention to the y axis range of the two graphs; c) orientation distribution function using the standard deviations specified in the corresponding legend

the value of standard deviation. Figure 6 shows the calculated reflectance spectra for the applied sample using standard deviation equal to 1° and 15°. The logistic orientation distribution functions for the variances 1°, 3° and 15° are also illustrated in the same figure, to show the broadness of the pigment tilt angle in such conditions. Reflectance factor spectra show that smaller variance results in significant reflection only at reflectance angles close to the specular reflection, at −30° and −60°. Other angles have very low reflectance factor. When orientation distribution is broader (the standard deviation is bigger), the reflectance factor increases over a wide range of reflectance angles.

A small standard deviation means that almost all flakes are parallel to the substrate, therefore the reflection of the sample is highly directional, and distributed around the specular direction, as a result of scattering on the edges of the flakes. A large standard deviation of the orientation distribution function means that the pigments are randomly oriented, thus reflect in accordance with these directions. The reflectance factor of such a coating becomes highly diffuse, meaning that a wider range of reflection directions reflect similar amount of light.

To analyse how the standard deviation of the orientation distribution function affects the reflectance factor at different reflectance angles, we have analysed the reflectance factor at λ = 650 nm as a function of the applied value of standard deviation. The results are shown in Figure 7. The reflectance factor at 650 nm is shown for all applied geometries plotted against standard deviation values between 1° and 40°.

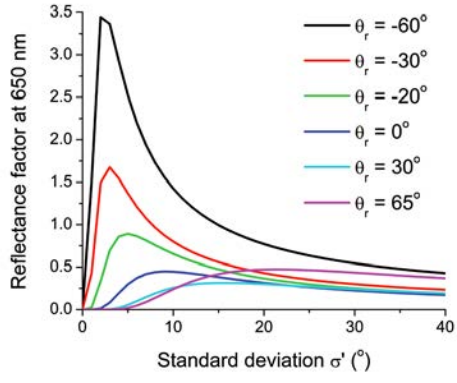

Figure 7: Reflectance factor at λ = 650 nm for specific reflectance angle versus standard deviation of orientation distribution function

The reflectance angles closer to the specular reflection have a quicker rise at small standard deviation and slowly converge to a constant value at larger standard deviation. The reflectance factor at angles furthest away from specular reflection, 30° and 65°, starts to increase at larger standard deviations, and does not show such a high reflectance factor like at angles closer to the specular direction. Such behaviour is in accordance with the logistic distribution function; when standard deviation becomes large enough, all inclination angles become possible.

5.3.2 Influence of orientation distribution's mean value

Here, we assume that the standard deviation is $\sigma' = 3°$, and we change the mean value of the logistic distribution function, θ_0'. If the flakes would be surrounded by air, the reflected angle for specular reflection on flakes (noted here as specular reflected angle) would be an addition of incident angle and flake's tilt angle. Because the flakes are inside a binder, the refraction at binder-air interface has to be also taken into account. The nonlinear relation between flake's tilt angle, θ_n', and specular reflected angle, is shown in Figure 8a. Flake's tilt angle can only range between −6° and 35°, beyond this we would encounter total internal reflection and no light would come from the sample. We can see that a small shift in flake's tilt angle causes a large shift in specular reflected angle.

Figure 8b shows the reflectance factor at $\lambda = 650$ nm at different reflectance angles, as a function of the applied mean value, ranging from −6° to 35°. When we change the mean value, we see that every aspecular angle has its own reflectance factor peak. The position of these peaks is directly related to the specular reflected angle, shown in Figure 8a. The intensity of the peaks, on the other hand, is mainly related to the denominator in Equation [3], where we have cosine of flake tilt angle and reflected angle (Figure 8c). This part of the equation is relatively low for most of the angles, but becomes large in the border range of flake tilt angles, corresponding to aspecular angles −60° and 65°. This explains the much higher intensity of reflectance factor peaks for those two aspecular angles in relation to other aspecular angles.

5.4 Influence of the substrate

The influence of the substrate can be analysed when different paper substrates are used. We have used black, magenta, cyan and yellow paper substrate (Figure 9). To show the corresponding effects, we calculated reflectance factor spectra of the effect coating with different surface coverage, C. Figure 10 is showing the results for $C = 0.1$, 0.5 and 0.9 for reflectance angle 60°. Other parameters used in the calculations were those defined in Table 2. Figure 10 should be compared with Figure 5, where the same parameters were used with white paper substrate.

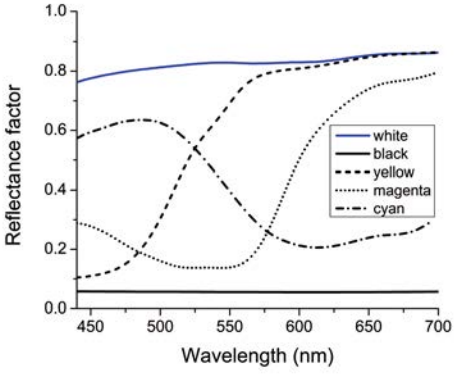

Figure 9: Measured reflectance factor for white, black, magenta, cyan and yellow paper substrates

Even with high surface coverage, $C = 0.9$, some differences were obtained in calculated spectra when different paper substrates were applied. Coating on magenta and yellow substrates that have high reflectance factor at $\lambda > 550$ nm, where the flakes also give high reflectance, give similar but slightly lower reflectance as the white substrate. Cyan and black paper substrates give even smaller reflectance factor values since the reflectance of

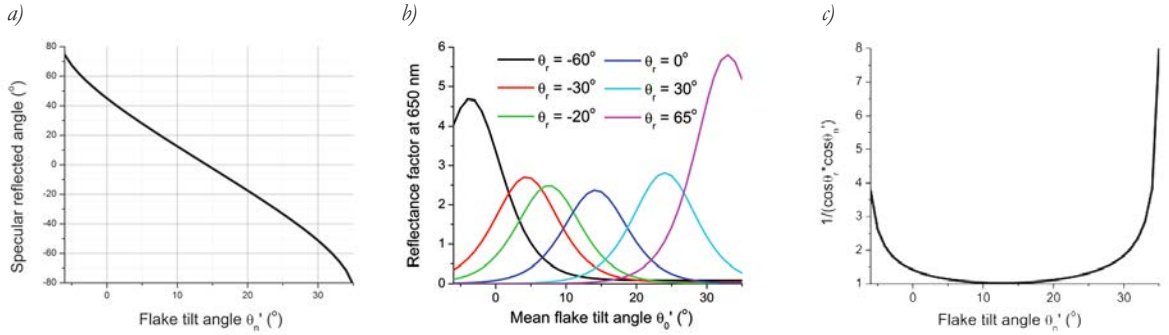

Figure 8: a) The reflected angle for specular reflection on flakes (specular reflected angle) as a function of flake tilt angle, b) reflectance factor at $\lambda = 650$ nm for specific reflectance angle as a function of orientation distribution's mean value, θ_0', and c) inverse of cosine of flake tilt and reflected angle versus flake tilt angle

the substrate alone is not high in that region. The small difference is because the interference effect caused by the pigments produces much higher reflectance factor values than the reflection from the substrate. When the surface coverage is getting smaller, the difference among paper substrates becomes larger. This is expected, since more and more of the substrate is visible and thus it contributes more to the reflectance factor of the entire coating. Not only the reflectance factor intensity changes, but also the shape of the reflectance factor curve starts to change and becomes more and more similar to the reflection of the substrate alone (Figure 9).

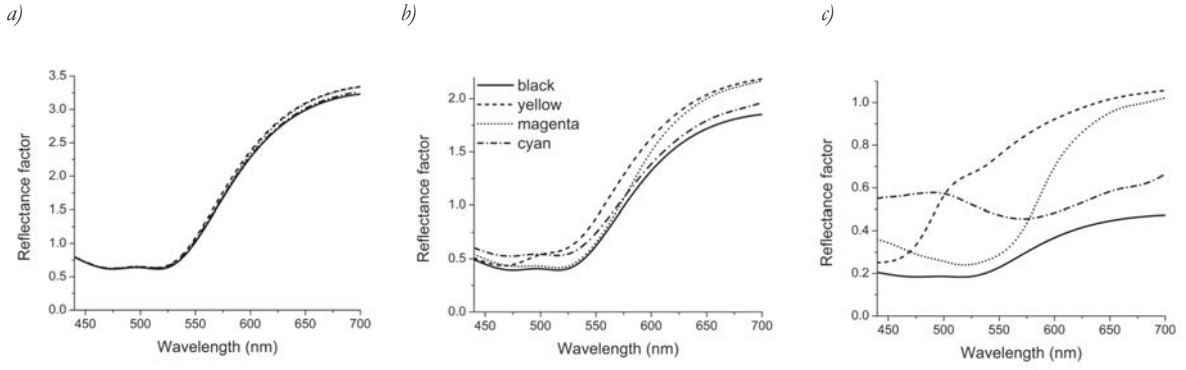

Figure 10: Reflectance factor calculated for the reflection angle −60° using surface coverage a) C = 0.9, b) C = 0.5, and c) C = 0.1 for different paper substrates (the legend in the middle graph applies to all three graphs); other parameters used in the calculation are those from Table 2; scale on y axis is changing for different C parameter, however, the same C parameter has the same y axis scale in this Figure 10 as well as in Figure 5

6. Conclusions

The focus of this research is on modelling the reflectance spectra of the selected special effect coating with interference pigments, having a Fe_2O_3 layer on a mica core. The modelled reflectance factor was validated with measurements of the selected sample at the same goniometric angles that were used in the model. The influence of three important parameters on goniometric reflectance factor was analysed, namely surface coverage, pigment orientation distribution and coating substrate. Surface coverage is directly related to the diameter and volume concentration of pigments for a given pigment thickness, i.e. aspect ratio, and both can be varied in the ink or paint manufacturing process. Depending on this factor, the coating substrate will affect the reflectance factor and influence the appearance of the coating. The pigment orientation distribution is an important factor when applying the ink or paint. Different application processes can distribute pigments with different orientation and standard deviation of orientation, and, as we have shown, this parameter can have great influence on the goniometric reflectance factor. Substrate used for application of the coating also contributes to the overall appearance of the sample, especially if the surface coverage is small. The results of our research show that the model built for such samples provides useful results; therefore it will be developed further. The coating sample, selected to present the application of the numerical model, includes all types of optical events taken into account in our numerical model. Therefore, this evaluation shows that the model is generally acceptable for effect coatings with both types of flakes, class (i) and class (ii). Moreover, this makes a good ground for further research of problems connected with appearance of gonioapparent samples. Moreover, interference flakes with more layers (multilayered interference flakes) are currently being considered. The entire data will be used to check the possibility of using the numerical model to define the input data for appearance fingerprinting.

The entire research has an ambition to provide a generalized model for goniospectrometric reflectance factor of effect coatings with arbitrary complexity. The numerical model should help in answering the question which spatial resolution is good enough to describe the BRDF of effect coatings. While coatings with all currently known special effects pigments will be considered, the proposed model will provide the reflection spectrum for arbitrary illumination–viewing directions for any combinations of ink/paint preparation and coating application. Such data are important for several purposes of optically complex coatings, being for decorative, security or any other purpose.

Acknowledgements

The authors acknowledge X-Rite and their country representative, Roman Habicht, for the opportunity to apply the software of the MA98 multi-angle spectrophotometer, and to Hana Erznožnik and Frenk Šemen at Helios d. d., Slovenia, for measurements on their apparatus.

References

ASTM, 2001. ASTM E2175-01, *Standard practice for specifying the geometry of multiangle spectrophotometers*. Conshohocken, PA, USA: ASTM International.

Database of Optical Constants for Cosmic Dust, 2015. Laboratory Astrophysics Group, University of Jena, Germany. Available at: <http://www.astro.uni-jena.de/Laboratory/OCDB/> [Accessed 10 August 2015].

Germer, T.A. and Nadal, M.E., 2001. Modeling the appearance of special effect pigment coatings. In: Z.-H., Gu and A.A., Maradudin,, eds. *SPIE Proceedings* Vol. 4447, pp. 77–86.

Germer, T.A., Zwinkels, J.C. and Tsai, B.K., eds., 2014. Spectrophotometry: accurate measurement of optical properties of materials. *Experimental Methods in the Physical Sciences*, 46.

Goldstein, D., 2003. *Polarized Light, Second Edition Revised and Expanded*. New York: Marcel Dekker, Inc.

Kasarova, S.N., Sultanova, N.G., Ivanov, C.D. and Nikolov, I.D., 2007. Analysis of the dispersion of optical plastic materials, *Optical Materials*, 29(11), pp. 1481–1490.

Kirchner, E. and Houweling, J., 2009. Measuring flake orientation for metallic coatings. *Progress in Organic Coating*, 64, pp. 287–293.

Kirchner, E. and Cramer, W., 2012. Making sense of measurement geometries for multi-angle spectrophotometers. *Color Research and Application*, 37(3), pp. 186–198.

Klanjšek Gunde, M. and Rogelj, N., 2013, Suitability of goniospectrophotometric space curves as appearance fingerprints, *Applied Optics*, 52(12), pp. 2718–2728.

Maile, F.J., Pfaff, G. and Reynders, P., 2005. Effect pigments – past, present and future. *Progress in Organic Coatings*, 54(3), pp. 150–163.

MERCK, 2012, *Safety data sheet, Irodin 4504 Lava Red*. Available at: <http://merck-performance-materials.com/> [Accessed 10 August 2015].

Palik, E.D., ed., 1997. *Handbook of Optical Constants of Solids*. San Diego, Chestnut Hill, London: Academic Press.

Pfaff, G. and Reynders, P., 1999. Angle-dependent optical effects deriving from submicron structures of films and pigments. *Chemical Reviews*, 99(7), pp. 1963–1982.

Rogelj, N., Poberaj I. and Klanjšek Gunde, M., 2013. Goniospectrophotometric space curves of diffraction gratings and their applicability as appearance fingerprints. *Applied Optics*, 52(34), pp. 8355–8362.

Schanda, J., ed., 2007. *Colorimetry: Understanding the CIE System*. Hoboken, New Jersey: John Wiley & Sons.

Takagi, A., Watanabe, A. and Baba, G., 2005. Prediction of spectral reflectance factor distribution of automotive paint finishes. *Color Research and Application*, 30(4), pp. 30, 275–282.

Takagi, A., Sato, S. and Baba, G., 2007. Prediction of spectral reflectance factor distribution of color-shift paint finishes. *Color Research and Application*, 32(5), pp. 378–387.

Torrance, K.E. and Sparrow, E.M., 1967. Theory for off-specular reflection from roughened surfaces. *Journal of the Optical Society of America*, 57(9), pp. 1105–1114.

X-Rite, 2010. *X-Rite MA98: Portable multi-angle spectrophotometers*, X-Rite, Incorporated. Available at: <https://www.xrite.com/documents/literature/en/L10-372_MA98_en.pdf> [Accessed 10 August 2015].